

Relativistic coupled-cluster study of RaF as a candidate for the parity- and time-reversal-violating interaction

Sudip Sasmal,¹ Himadri Pathak,¹ Malaya K. Nayak,² Nayana Vaval,¹ and Sourav Pal³

¹*Electronic Structure Theory Group, Physical Chemistry Division, CSIR-National Chemical Laboratory, Pune 411008, India*

²*Theoretical Chemistry Section, Bhabha Atomic Research Centre, Trombay, Mumbai 400085, India*

³*Department of Chemistry, Indian Institute of Technology Bombay, Powai, Mumbai 400076, India*

(Received 11 March 2016; published 9 June 2016)

We have employed both the Z -vector method and the expectation-value approach in the relativistic coupled-cluster framework to calculate the scalar-pseudoscalar (S-PS) \mathcal{P}, \mathcal{T} -odd interaction constant W_s and the effective electric field E_{eff} experienced by the unpaired electron in the ground electronic state of RaF. Further, the magnetic hyperfine structure constants of ^{223}Ra in RaF and $^{223}\text{Ra}^+$ are also calculated and compared with the experimental values wherever available to judge the extent of the accuracy obtained with the employed methods. The outcome of our study reveals that the Z -vector method is superior to the expectation-value approach in terms of accuracy obtained for the calculation of ground-state property. The Z -vector calculation shows that RaF has a high E_{eff} (52.5 GV/cm) and W_s (141.2 kHz), which makes it a potential candidate for the electric dipole moment of the electron (eEDM) experiment. An estimation of uncertainty associated with our final results is made, and it is found that it lies below 10%.

DOI: [10.1103/PhysRevA.93.062506](https://doi.org/10.1103/PhysRevA.93.062506)

I. INTRODUCTION

The ongoing accelerator-based experiments in the search for new physics could solve some of the unanswered problems of fundamental physics like matter-antimatter asymmetry. A complement to these high-energy experiments is the search for violation in spatial inversion (\mathcal{P}) and time-reversal (\mathcal{T}) symmetries in nuclei, atoms, or molecules in the low-energy domain using nonaccelerator experiments [1–7]. One such \mathcal{P}, \mathcal{T} -violating interaction results in the electric dipole moment of the electron (eEDM) [8–11]. The eEDM predicted by the standard model (SM) of elementary particle physics is too small ($<10^{-38} e \text{ cm}$) [12] to be observed by current experiments. However, many extensions of the SM predict the value of eEDM to be in the range of 10^{-26} – $10^{-29} e \text{ cm}$ [13], and the sensitivity of the modern eEDM experiment also lies in the same range. Until now, the experiment done by the ACME collaboration [11] using ThO has yielded the best upper bound limit of eEDM. The high sensitivity of the modern eEDM experiment is mainly due to the fact that heavy paramagnetic diatomic molecules offer a very high internal effective electric field E_{eff} , which enhances the eEDM effects [14,15]. In the experiment, both eEDM and the coupling interaction between the scalar-hadronic current and the pseudoscalar electronic current contribute to the \mathcal{P}, \mathcal{T} -odd frequency shift. Therefore, it is impossible to decouple the individual contribution from these two effects in a single experiment. However, it is possible to untwine these two contributions from each other, and an independent limit on the value of eEDM d_e and scalar-pseudoscalar (S-PS) coupling constant k_s can be obtained by using data from two different experiments, as suggested by Dzuba *et al.* [16]. Therefore, accurate values of E_{eff} and the S-PS \mathcal{P}, \mathcal{T} -odd interaction constant W_s are needed since these two quantities cannot be measured by means of any experiment. Therefore, one has to rely on an accurate *ab initio* theory that can simultaneously take care of the effects of relativity and electron correlation for the calculation of these quantities.

The best way to include the effects of special relativity in the electronic structure calculations is to solve the Dirac-Hartree-Fock (DHF) equation in the four-component framework. The DHF method considers an average electron-electron interaction and thus misses the correlation between electrons having the same spin. On the other hand, the single-reference coupled-cluster (SRCC) method is the most preferred many-body theory to incorporate the dynamic part of the electron correlation. The calculation of properties in the SRCC framework can be done either numerically or analytically. In the numerical method [also known as the finite-field (FF) method], the coupled-cluster amplitudes are functions of the external field parameters [17], and thus, for the calculations of each property, a separate set of CC calculations is needed. The error associated with the FF method is also dependent on the method of calculation, i.e., the number of data points considered for the numerical differentiation. On the contrary, in the analytical method, the CC amplitudes are independent of the external field of perturbation, and therefore, one needs to solve only one set of CC equations to calculate any number of properties. The normal CC (NCC) method, being nonvariational, does not satisfy the generalized Hellmann-Feynman (GHF) theorem, and thus, the expectation value and the energy derivative approach are two different formalisms to calculate first-order properties. However, the energy derivative in the NCC framework is the corresponding expectation value plus some additional terms, which make it closer to the property value obtained in the full configuration interaction (FCI) method. Thus, the property value obtained in the energy-derivative method is much more reliable than the corresponding expectation-value method. Another disadvantage of the expectation-value method is that it leads to a nonterminating series, and any truncation further introduces an additional error. The Z -vector method [18,19] (an energy-derivative method), on the other hand, leads to a naturally terminating series at any level of approximation. The higher-order derivative in the NCC

framework can be calculated by using the Lagrange multiplier method [20], and for the first-order energy derivative, it leads to equations identical to those of the Z -vector method. It is worth noting that there are alternative options like expectation-value CC (XCC) [21,22], unitary CC (UCC) [23,24], and extended CC (ECC) [25–27] to solve the SRCC equation. All these methods are known in the literature as the variational coupled-cluster (VCC) method [28]. These VCC methods are well established in the nonrelativistic framework but are not very popular in the relativistic domain; a few are documented in the literature, such as relativistic UCC by Sur *et al.* [29,30], which is applicable only for the purpose of atomic calculations. Recently, Sasmal *et al.* implemented ECC in the four-component relativistic domain to calculate the magnetic hyperfine structure (HFS) constants of both atoms and molecules in their open-shell ground-state configuration [31]. Because the ECC method is variational, it satisfies the GHF theorem; therefore, the expectation value and the energy-derivative approach are identical to each other. However, in the ECC method amplitude equations for the excitation and deexcitation operators are coupled to each other, whereas in the Z -vector method, the amplitude equations of the excitation operator are decoupled from the amplitude equations of the deexcitation operator. This accelerates the convergence in the Z -vector method with a lower computational cost than the ECC.

In this work, we have calculated E_{eff} and W_s of RaF in its ground electronic ($^2\Sigma$) state using the Z -vector method in the CC framework. We also calculated these properties in the expectation-value method to show the superiority of the Z -vector method over the expectation-value method. We have chosen the RaF molecule for the following reasons: This molecule has been proposed for the \mathcal{P} -odd and \mathcal{P},\mathcal{T} -odd experiment [32–34] due to its high Schiff moment, E_{eff} , and W_s . The E_{eff} of the $^2\Sigma$ state of RaF is even higher than the ground state ($^2\Sigma$) of YbF. Therefore, more precise values of E_{eff} and W_s and their ratio are very important for the eEDM experiment using this molecule. RaF can be directly laser cooled as it has a high diagonal Franck-Condon matrix element between the ground state and first excited electronic state, and the corresponding transition frequency lies in the visible region with a reasonable lifetime [32].

This paper is organized as follows. A brief overview of the expectation-value and the Z -vector methods in the CC framework, including concise details of the properties calculated in this work, is given in Sec. II. Computational details are given in Sec. III. We present our calculated results and discuss them in Sec. IV before making concluding remarks. Atomic units are used consistently unless stated otherwise.

II. THEORY

A. Expectation value and Z -vector method

The DHF wave function is the best description of the ground state in a single-determinant theory, and thus, it is used as a reference function for the correlation calculations where the Dirac-Coulomb (DC) Hamiltonian is used, which is

given by

$$H_{DC} = \sum_i \left[-c(\vec{\alpha} \cdot \vec{\nabla})_i + (\beta - \mathbb{1}_4)c^2 + V^{\text{nuc}}(r_i) + \sum_{j>i} \frac{1}{r_{ij}} \mathbb{1}_4 \right]. \quad (1)$$

Here, α and β are the usual Dirac matrices, c is the speed of light, $\mathbb{1}_4$ is the 4×4 identity matrix, and the sum is over all the electrons, which is denoted by i . The Gaussian charge distribution is used as the nuclear potential function $V^{\text{nuc}}(r_i)$. The DHF method approximates the electron-electron repulsion in an average way and thus misses the correlation between same-spin electrons. In this article, we have used the SRCC method to incorporate the dynamic part of the electron correlation. The SRCC wave function is given by $|\Psi_{cc}\rangle = e^T |\Phi_0\rangle$, where Φ_0 is the DHF wave function and T is the coupled-cluster excitation operator, which is given by

$$T = T_1 + T_2 + \dots + T_N = \sum_n^N T_n, \quad (2)$$

with

$$T_m = \frac{1}{(m!)^2} \sum_{ij\dots ab\dots} t_{ij\dots}^{ab\dots} a_a^\dagger a_b^\dagger \dots a_j a_i, \quad (3)$$

where i, j (a, b) are the hole (particle) indices and $t_{ij\dots}^{ab\dots}$ are the cluster amplitudes corresponding to the cluster operator T_m . In the coupled-cluster with single and double excitations (CCSD) model, $T = T_1 + T_2$. The equations for T_1 and T_2 are given by

$$\langle \Phi_i^a | (H_N e^T)_c | \Phi_0 \rangle = 0, \quad \langle \Phi_{ij}^{ab} | (H_N e^T)_c | \Phi_0 \rangle = 0, \quad (4)$$

where H_N is the normal ordered (DC) Hamiltonian and the subscript c means only the connected terms exist in the contraction between H_N and T . Size extensivity is ensured by this connectedness.

Once the cluster amplitudes are solved, the expectation value of any property operator of interest $\langle O_N \rangle$ can be calculated by the following expression, as given in Refs. [35,36]:

$$\begin{aligned} \langle O_N \rangle &= \frac{\langle \Psi_{cc} | O_N | \Psi_{cc} \rangle}{\langle \Psi_{cc} | \Psi_{cc} \rangle} = \frac{\langle \Phi_0 e^{T^\dagger} | O_N | e^T \Phi_0 \rangle}{\langle \Phi_0 | e^{T^\dagger} e^T | \Phi_0 \rangle} \\ &= \langle \Phi_0 | (e^{T^\dagger} O_N e^T)_c | \Phi_0 \rangle. \end{aligned} \quad (5)$$

The above series is a nonterminating series. Since the dominant contribution comes from the linear terms, the linear approximation is the most favored choice. A detailed diagrammatic expression considering only linear terms within the CCSD approximation is given in Fig. 1, and the corresponding algebraic equation is given in Eq. (6). We have used Einstein's summation convention; that is, the repeated indices are summed over in the expression. The t amplitudes with particle (hole) indices in the subscript (superscript) are the corresponding amplitudes of the T^\dagger operator. It is interesting to note that there is no possible diagram (or algebraic expression) for $T_2^\dagger O$ or $O T_2$ since closed connected diagrams cannot be

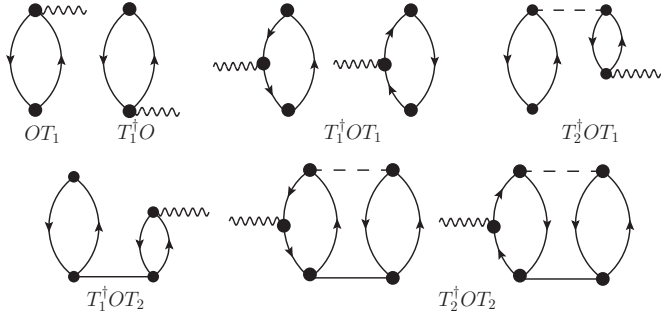


FIG. 1. Diagrams of the expectation-value approach using the linear truncation scheme.

constructed by these two expressions.

$$\begin{aligned} \langle O \rangle &= O(i,a)t_i^a + t_a^i O(a,i) + t_a^i O(a,b)t_i^b - t_a^i O(j,i)t_j^a \\ &+ t_{ab}^{ij} O(b,j)t_i^a + t_a^i O(j,b)t_{ij}^{ab} \\ &- \frac{1}{2} t_{ab}^{ij} O(k,j)t_{ik}^{ab} + \frac{1}{2} t_{ab}^{ij} O(b,c)t_{ij}^{ac}. \end{aligned} \quad (6)$$

The CC amplitudes are solved in a nonvariational way [using Eq. (4)], and thus, the CC energy is not minimized with respect to the determinantal coefficient and the molecular orbital coefficient in the expansion of the many-electron correlated wave function for a fixed nuclear geometry [17]. Therefore, the calculation of the CC energy derivative needs to include the derivative of the energy with respect to these two coefficients in addition to the derivative of these two parameters with respect to the external field of perturbation.

However, the derivative terms associated with the determinantal coefficient can be integrated by the introduction of a perturbation-independent linear operator Λ [19]. Λ is an antisymmetrized deexcitation operator whose second quantized form is given by

$$\Lambda = \Lambda_1 + \Lambda_2 + \dots + \Lambda_N = \sum_n \Lambda_n, \quad (7)$$

where

$$\Lambda_m = \frac{1}{(m!)^2} \sum_{ij \dots ab \dots} \lambda_{ab \dots}^{ij \dots} a_i^\dagger a_j^\dagger \dots a_b a_a, \quad (8)$$

where $\lambda_{ab \dots}^{ij \dots}$ are the cluster amplitudes corresponding to the operator Λ_m . A detailed description of the Λ operator and the amplitude equation is given in Ref. [19]. In the CCSD model, $\Lambda = \Lambda_1 + \Lambda_2$. The explicit equations for the amplitudes of the Λ_1 and Λ_2 operators are given by

$$\langle \Phi_0 | [\Lambda(H_N e^T)_c]_c | \Phi_i^a \rangle + \langle \Phi_0 | (H_N e^T)_c | \Phi_i^a \rangle = 0, \quad (9)$$

$$\begin{aligned} &\langle \Phi_0 | [\Lambda(H_N e^T)_c]_c | \Phi_{ij}^{ab} \rangle + \langle \Phi_0 | (H_N e^T)_c | \Phi_{ij}^{ab} \rangle \\ &+ \langle \Phi_0 | (H_N e^T)_c | \Phi_i^a \rangle \langle \Phi_i^a | \Lambda | \Phi_{ij}^{ab} \rangle = 0. \end{aligned} \quad (10)$$

It is interesting to note that the third term of Eq. (10) is of the nature of the disconnected type and it eventually produces one disconnected diagram in the Λ_2 amplitude equation (for details see Refs. [19,37]). Although the diagram is disconnected, it does not have any closed parts. This ensures that the

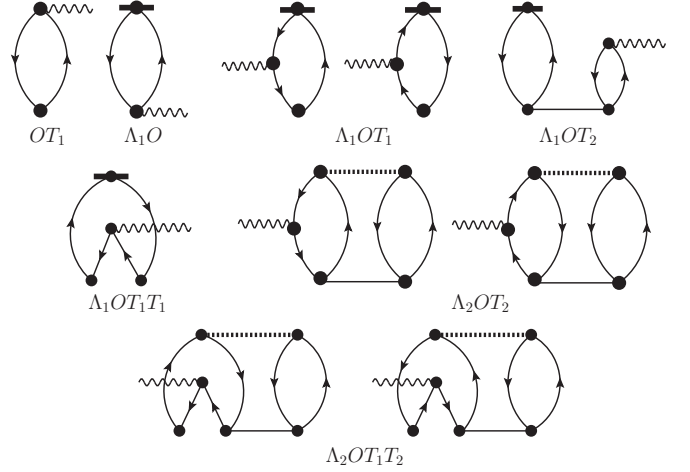


FIG. 2. Diagrams of the energy derivative in the Z-vector method.

corresponding energy diagram is linked, which restores the size extensivity. The energy derivative can be given as

$$\Delta E' = \langle \Phi_0 | (O_N e^T)_c | \Phi_0 \rangle + \langle \Phi_0 | [\Lambda(O_N e^T)_c]_c | \Phi_0 \rangle, \quad (11)$$

where O_N is the derivative of the normal ordered perturbed Hamiltonian with respect to the external field of perturbation. A detailed diagrammatic expression is given in Fig. 2, and the corresponding algebraic equation is given by

$$\begin{aligned} \Delta E' &= O(i,a)t_i^a + \lambda_a^i O(a,i) + \lambda_a^i O(a,b)t_i^b + \lambda_a^i O(j,i)t_j^a \\ &+ \lambda_a^i O(j,b)t_{ij}^{ab} - \lambda_a^i O(j,b)t_i^b t_j^a - \frac{1}{2} \lambda_{ab}^{ij} O(k,j)t_{ik}^{ab} \\ &+ \frac{1}{2} \lambda_{ab}^{ij} O(b,c)t_{ij}^{ac} - \frac{1}{2} \lambda_{bc}^{ik} O(j,a)t_i^a t_{jk}^{bc} \\ &- \frac{1}{2} \lambda_{ac}^{jk} O(i,b)t_i^a t_{jk}^{bc}. \end{aligned} \quad (12)$$

B. One-electron property operators

E_{eff} can be obtained by evaluating the following matrix element:

$$E_{\text{eff}} = |W_d \Omega| = \left| \langle \Psi_\Omega | \sum_j \frac{H_d(j)}{d_e} | \Psi_\Omega \rangle \right|, \quad (13)$$

where Ω is the component of total angular momentum along the molecular axis and Ψ_Ω is the wave function corresponding to the Ω state. n is the total number of electrons, and H_d is the interaction Hamiltonian of d_e with the internal electric field and is given by [38,39],

$$H_d = 2icd_e \gamma^0 \gamma^5 p^2, \quad (14)$$

where γ are the usual Dirac matrices and p is the momentum operator.

The matrix element of the scalar-pseudoscalar \mathcal{P}, \mathcal{T} -odd interaction constant W_s is given by

$$W_s = \frac{1}{\Omega k_s} \langle \Psi_\Omega | \sum_j H_{\text{SP}}(j) | \Psi_\Omega \rangle, \quad (15)$$

where k_s is the dimensionless electron-nucleus scalar-pseudoscalar coupling constant, which is defined as $Zk_s = (Zk_{s,p} + Nk_{s,n})$, where $k_{s,p}$ and $k_{s,n}$ are electron-proton and electron-neutron coupling constants, respectively.

The interaction Hamiltonian is defined as [40]

$$H_{SP} = i \frac{G_F}{\sqrt{2}} Z k_s \gamma^0 \gamma^5 \rho_N(r), \quad (16)$$

where $\rho_N(r)$ is the nuclear charge density normalized to unity and G_F is the Fermi constant. The calculation of the above matrix elements depends on an accurate wave function in the core (near-nuclear) region, and the standard way to determine the accuracy of the electronic wave function in that region is to compare the theoretically calculated HFS constant with the experimental value. The magnetic hyperfine constant of the J th electronic state of an atom is given by

$$A_J = \frac{\vec{\mu}_k}{IJ} \langle \Psi_J | \sum_i \left(\frac{\vec{\alpha}_i \times \vec{r}_i}{r_i^3} \right) | \Psi_J \rangle, \quad (17)$$

where Ψ_J is the wave function of the J th electronic state, I is the nuclear spin quantum number, and $\vec{\mu}_k$ is the magnetic moment of the nucleus k . For a diatomic molecule, The parallel (A_{\parallel}) and perpendicular (A_{\perp}) magnetic hyperfine constants of a diatomic molecule can be written as

$$A_{\parallel(\perp)} = \frac{\vec{\mu}_k}{I\Omega} \langle \Psi_{\Omega} | \sum_i \left(\frac{\vec{\alpha}_i \times \vec{r}_i}{r_i^3} \right)_{z(x/y)} | \Psi_{\Omega(-\Omega)} \rangle, \quad (18)$$

where the value of Ω is 1/2 for the ground electronic state ($^2\Sigma$) of RaF.

III. COMPUTATIONAL DETAILS

A locally modified version of the DIRAC10 [41] program package is used to solve the DHF equation and to construct the one-body and two-body matrix elements and the one-electron property integrals of interest. The finite size of a nucleus with a Gaussian charge distribution is considered as the nuclear model, where the nuclear parameters [42] are set to the default values in DIRAC10. Small-component basis functions are generated from the large component by applying the restricted kinetic balance (RKB) [43] condition. The basis functions are represented in a scalar basis, and unphysical

solutions are removed by means of the diagonalization of the free-particle Hamiltonian. This generates the electronic and positronic solutions in a 1:1 manner. In our calculations, we have used the following uncontracted basis sets: in the triple zeta (TZ) basis, dyall.cv3z [44] for Ra and cc-pCVTZ [45] for F, and in the quadruple zeta (QZ) basis, dyall.cv4z [44] for Ra and cc-pCVQZ [45] for F. In the TZ basis, three calculations are done for the magnetic HFS constant of Ra^+ by using 51, 69, and 87 correlated electrons, and these are denoted by A, B, and C, respectively. In the QZ basis, three more calculations are done by using 51, 69, and 87 correlated electrons, and these are denoted by D, E, and F, respectively. The properties of RaF are calculated using two different bases. In the TZ basis, three calculations are done by using 61, 79, and 97 correlated electrons, and those are denoted by G, H, and I, respectively, and similarly, in the QZ basis, the calculations using 61, 79, and 97 correlated electrons are denoted by J, K, and L, respectively. The bond length of RaF is taken as $4.23a_0$ (2.24 \AA) [34] in all our calculations.

IV. RESULTS AND DISCUSSION

The aim of the present study is to exploit the RaF molecule for the eEDM experiment and to provide more accurate values of the \mathcal{P}, \mathcal{T} -odd interaction constants of RaF. Since there are no experimental analogs of the \mathcal{P}, \mathcal{T} -odd interaction constants like E_{eff} and W_s , the accuracy of these theoretically obtained quantities can be assessed by comparing the theoretically obtained HFS values with the corresponding experimental values. Unfortunately, the experimental HFS results of Ra in RaF are not available. Therefore, we compare the experimental HFS value of $^{223}\text{Ra}^+$ [46,47] with the value obtained by theory using the same basis of Ra as used for the calculation of RaF.

In Table I, we present the information regarding the employed basis sets, the cutoff used for occupied and virtual orbitals, and the number of active spinors for the correlation calculation. We also compiled the correlation energy obtained from second-order many-body perturbation theory [MBPT(2)] and the CCSD method.

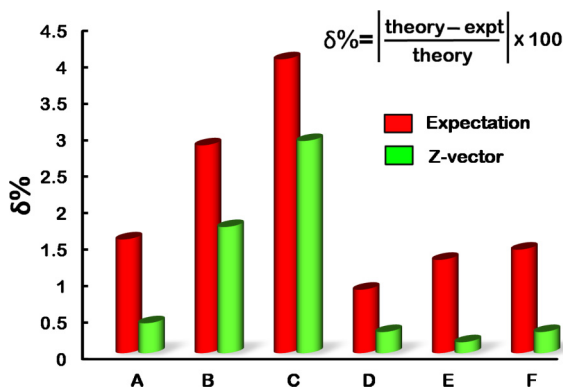
TABLE I. Cutoff used and correlation energy of the ground state of Ra^+ and RaF in different basis sets.

Name	Nature	Basis		Cutoff (a.u.)		Spinor		Correlation energy (a.u.)	
		Ra	F	Occupied	Virtual	Occupied	Virtual	MBPT(2)	CCSD
Ra⁺									
A	TZ	dyall.cv3z		-30	500	51	323	-1.74841495	-1.57235409
B	TZ	dyall.cv3z		-130	500	69	323	-2.42790147	-2.20700361
C	TZ	dyall.cv3z			500	87	323	-2.78897499	-2.55468917
D	QZ	dyall.cv4z		-30	20	51	349	-1.43221422	-1.31515023
E	QZ	dyall.cv4z		-130	20	69	349	-1.49747209	-1.37242346
F	QZ	dyall.cv4z			20	87	349	-1.50382815	-1.37827038
RaF									
G	TZ	dyall.cv3z	cc-pCVTZ	-30	500	61	415	-2.09671991	-1.91684123
H	TZ	dyall.cv3z	cc-pCVTZ	-130	500	79	415	-2.77624243	-2.55153111
I	TZ	dyall.cv3z	cc-pCVTZ		500	97	415	-3.13733209	-2.89923481
J	QZ	dyall.cv4z	cc-pCVQZ	-30	20	61	449	-1.76368821	-1.63988444
K	QZ	dyall.cv4z	cc-pCVQZ	-130	20	79	449	-1.82908547	-1.69728677
L	QZ	dyall.cv4z	cc-pCVQZ		20	97	449	-1.83544557	-1.70314714

TABLE II. Magnetic hyperfine coupling constant (in MHz) of $^{223}\text{Ra}^+$.

Basis	Expectation	Z vector	Expt. [46,47]
A	3458	3418	
B	3504	3464	
C	3547	3506	3404(2)
D	3434	3394	
E	3448	3409	
F	3453	3414	

In Table II, we present the ground state (2S) magnetic HFS constant value of $^{223}\text{Ra}^+$ using both expectation-value and Z-vector methods. Our results are compared with the available experimental value [46,47]. The deviations of the Z vector and expectation values from the experiment are presented in Fig. 3. It is clear that the deviations of the expectation-value method are always greater than those of the Z-vector method. This is expected because the Z vector is a better method than the expectation-value method for the ground-state property; in fact, the Z-vector value is the corresponding expectation value plus some additional terms which make it closer to the FCI property value. It is interesting to note that when we go from the TZ to QZ basis with the same number of correlated electrons (i.e., from A to D, B to E, and C to F), the relative deviation of both the Z vector and expectation value decreases. This is because QZ, in comparison to TZ, further improves the configuration space by adding one higher angular momentum basis function. It is also interesting to see that in the TZ basis, if we go from A to B and B to C, the addition of 18 electrons ($4s + 3d + 4p$ and $1s-3p$) changes the Z-vector HFS constant by 46 and 42 MHz. Similarly, in the QZ basis, as we go from D to E and E to F, the addition of 18 electrons changes the Z-vector HFS constant by 15 and 5 MHz. From this observation, we can note that the core polarization plays a definite role in the correlation contribution of the HFS constant and the effect is severe for lower basis sets. Further, the enlargement of the basis set and the addition of core electrons have opposite effects in the calculated HFS value of Ra^+ . However, The magnetic HFS constant obtained in the all-electron Z-vector calculation using

FIG. 3. Comparison of relative deviations between the expectation-value and Z-vector results of the magnetic HFS constant of $^{223}\text{Ra}^+$.TABLE III. Molecular dipole moment μ and magnetic HFS constants of ^{223}Ra in RaF. Expect. = expectation value.

Basis	μ (D)		A_{\perp} (MHz)		A_{\parallel} (MHz)	
	Expect.	Z vector	Expect.	Z vector	Expect.	Z vector
G	3.7059	3.7220	2031	1987	2123	2078
H	3.7028	3.7207	2059	2014	2152	2107
I	3.7017	3.7201	2084	2038	2178	2132
J	3.8404	3.8474	2029	1982	2119	2072
K	3.8375	3.8459	2037	1991	2128	2082
L	3.8374	3.8459	2040	1993	2131	2085

the QZ basis (basis F) is very close to the experimental value ($\delta\% = 0.29$).

The properties described by Eqs. (13), (15), and (18) strongly depend on the electronic configuration of the given (heavy) atom and are also known as atom-in-compound (AIC) properties [48]. The accuracy of the theoretically calculated AIC properties depends on the accurate evaluation of the electron density near the atomic core region. From the accuracy of our calculated HFS constant of Ra^+ ($\delta\% = 0.29$), we can note that the all-electron Z-vector calculation produces an accurate wave function in the vicinity of the Ra nucleus, and we also expect the same kind of accuracy for the RaF molecule.

We have calculated the molecular-frame dipole moment μ of RaF and perpendicular (A_{\perp}) and parallel (A_{\parallel}) magnetic HFS constants of ^{223}Ra in RaF using both expectation-value and Z-vector methods. The results are compiled in Table III. From Table III, it is clear that inclusion of more core electrons decreases the value of μ but increases the value of the magnetic HFS constants of ^{223}Ra in RaF. On the other hand, if we go from the TZ to QZ basis, the μ value is increased, but the magnetic HFS values are decreased. This observation shows that the increase of correlation space by either the addition of core electrons or higher angular momentum wave functions has an opposite effect on the near-nuclear and outer-region parts of the molecular wave function of RaF. We can also note that the enlargement of the basis set and core electrons has opposite effects in the properties of RaF.

In Table IV, we present the two \mathcal{P}, \mathcal{T} -odd interaction constants, namely E_{eff} and E_s . The E_{eff} value of RaF in the QZ basis using the all-electron Z-vector calculation (basis L) is 52.5 GV/cm. This E_{eff} value of RaF is even higher than the E_{eff} value of YbF in its ground state [49–54]. The W_s value of RaF

TABLE IV. \mathcal{P}, \mathcal{T} -odd interaction constants and their ratio of RaF. Expect. = expectation value.

Basis	W_s (kHz)		E_{eff} (GV/cm)		R ($10^{18} e^{-1} \text{cm}^{-1}$)	
	Expect.	Z vector	Expect.	Z vector	Expect.	Z vector
G	144.7	143.6	53.9	53.5	90.1	90.1
H	147.4	146.3	54.9	54.5	90.1	90.1
I	149.3	148.1	55.6	55.1	90.0	90.0
J	141.2	140.4	52.6	52.3	90.1	90.1
K	141.9	141.1	52.8	52.5	90.0	90.0
L	142.0	141.2	52.8	52.5	89.9	89.9

using the Z -vector method in the same basis (QZ, all electron) is 141.2 kHz. This high value of W_s suggests that the S-PS interaction will also be responsible for a significant change in the \mathcal{P}, \mathcal{T} -odd frequency shift in the eEDM experiment. These results reveal the possibility of using RaF in a future eEDM experiment. The ratio R of E_{eff} to W_s is also calculated as this is a very important quantity to obtain the independent limit of d_e and k_s by using two independent experiments. Our calculated value of R using the all-electron Z -vector method in the QZ (L) basis is 89.9 in units of $10^{18} e^{-1} \text{ cm}^{-1}$. Using this ratio, the relation of independent d_e and k_s with experimentally determined d_e^{expt} becomes (for more details see Ref. [55])

$$d_e + 5.56 \times 10^{-21} k_s = d_e^{\text{expt}}|_{k_s=0}, \quad (19)$$

where $d_e^{\text{expt}}|_{k_s=0}$ is the eEDM limit derived from the experimentally measured \mathcal{P}, \mathcal{T} -odd frequency shift at the limit $k_s = 0$.

The possible sources of error in our calculations are mainly from four sources: (i) higher-order relativistic effects (especially the Breit-Gaunt interaction) and nonadiabatic effects, (ii) incompleteness of the basis set, (iii) higher-order correlation effects, and (iv) the cutoff used for the virtual orbitals. Now, the AIC properties described here mainly depend on the electron density of the valence electron in the nuclear region, and thus, these types of properties are not very sensitive to the retardation and magnetic effects described by the Breit interaction [56,57]. The error associated with the nonadiabatic effects is also insignificant as the properties of a heavy diatomic molecule are calculated here. The error associated with the incompleteness of basis sets can be accessed by comparing our TZ and QZ results. The difference in all-electron correlation results of E_{eff} and W_s in the TZ and QZ bases is about 5%. The proper way to estimate the error associated with a missing correlation is to compare our results with the FCI or CCSD with partial triples [CCSD(T)] values. However, these types of calculations are very expensive and are beyond the scope of our present study. From our experience, we can state that the error associated with the missing higher-order correlation effects is about 3.5%. Therefore, considering all other sources of error, it can be assumed that the overall uncertainty in our final results is less than 10%.

We compare our calculated results with other theoretically obtained values in Table V. The first *ab initio* calculation of W_s of RaF was performed by Isaev *et al.* [33]. They employed the two-component zeroth-order regular approximation (ZORA) generalized Hartree-Fock (GHF) method and obtained a value of W_s of 150 kHz. They also obtained a value of E_{eff} of 45.5 GV/cm by using the ZORA-GHF value of W_s and the approximate ratio between E_{eff} and W_s . Kudashov *et al.* [34] employed two different methods to incorporate relativistic and electron correlation effects: (i) the spin-orbit direct configuration interaction (SODCI) method and (ii) the relativistic two-component Fock-space coupled-cluster approach (FS-RCC) within single- and double-excitation approximation.

TABLE V. Comparison of magnetic HFS constant (^{223}Ra), W_s , and E_{eff} of RaF.

Method	A_{\perp} (MHz)	A_{\parallel} (MHz)	W_s kHz	E_{eff} (GV/cm)
ZORA-GHF [33]	1860	1900	150	45.5
SODCI [34]	1720	1790	131	49.6
FS-RCC [34]	2020	2110	139	52.9
This work (QZ basis, all electron)				
Expectation value	2040	2131	142.0	52.8
Z vector	1993	2085	141.2	52.5

However, it is worth remembering that the truncated CI is not size extensive and thus cannot treat electron correlation properly, especially for a heavy electronic system like RaF, where the number of electrons is so large. In their FS-RCC method, Kudashov *et al.* [34] calculated the properties of RaF using the finite-field method, which is a numerical technique. They corrected the error associated with their calculation considering a higher-order correlation effect and basis set with the addition of a partial triple in the CCSD model [CCSD(T)] and using an enlarged basis set, respectively. On the other hand, we have calculated the property values of RaF via two analytical methods (expectation-value and Z -vector methods) in the relativistic coupled-cluster framework within the four-component formalism. We also calculated the E_{eff} and W_s values directly by using Eqs. (13) and (15), respectively.

V. CONCLUSION

In conclusion, we have applied both the Z -vector and expectation-value methods in the relativistic coupled-cluster framework to calculate parallel and perpendicular magnetic HFS constants of ^{223}Ra in RaF and E_{eff} and W_s of RaF. We have also calculated the magnetic HFS constant of $^{223}\text{Ra}^+$ to show the reliability of our results. Our most reliable values of E_{eff} and W_s of RaF are 52.5 GV/cm and 141.2 kHz, respectively, with an estimated uncertainty of less than 10%. This shows that RaF can be a potential candidate for the eEDM experiment. We also showed that core electrons play a significant role, and the effect is notable for lower basis sets. Our results also show that the Z vector, being an energy derivative method, is much more reliable than the expectation-value method.

ACKNOWLEDGMENTS

The authors acknowledge a grant from the CSIR 12th Five Year Plan project on Multi-Scale Simulations of Material (MSM) and the resources of the Center of Excellence in Scientific Computing at CSIR-NCL. S.S. and H.P. acknowledge support from the CSIR for their fellowship. S.P. acknowledges funding from a J. C. Bose Fellowship grant of the Department of Science and Technology (India).

[1] J. Ginges and V. Flambaum, *Phys. Rep.* **397**, 63 (2004).

[2] P. Sandars, *Phys. Lett.* **14**, 194 (1965).

[3] P. G. H. Sandars, *Phys. Rev. Lett.* **19**, 1396 (1967).

[4] L. N. Labzovskii, *Sov. Phys. JETP* **48**, 434 (1978).

- [5] L. M. Barkov, M. S. Zolotarev, and I. B. Khriplovich, *Sov. Phys. Usp.* **23**, 713 (1980).
- [6] F. L. Shapiro, *Sov. Phys. Usp.* **11**, 345 (1968).
- [7] M. Pospelov and A. Ritz, *Ann. Phys. (NY)* **318**, 119 (2005).
- [8] W. Bernreuther and M. Suzuki, *Rev. Mod. Phys.* **63**, 313 (1991).
- [9] B. C. Regan, E. D. Commins, C. J. Schmidt, and D. DeMille, *Phys. Rev. Lett.* **88**, 071805 (2002).
- [10] J. J. Hudson, D. M. Kara, I. J. Smallman, B. E. Sauer, M. R. Tarbutt, and E. A. Hinds, *Nature (London)* **473**, 493 (2011).
- [11] J. Baron *et al.*, *Science* **343**, 269 (2014).
- [12] I. B. Khriplovich and S. K. Lamoreaux, *CP Violation without Strangeness: The Electric Dipole Moments of Particles, Atoms, and Molecules* (Springer, London, 2011).
- [13] E. D. Commins, *Adv. At. Mol. Opt. Phys.* **40**, 1 (1999).
- [14] O. Sushkov and V. Flambaum, *J. Exp. Theor. Phys.* **48**, 608 (1978).
- [15] V. V. Flambaum, *Sov. J. Nucl. Phys.* **24**, 199 (1976).
- [16] V. A. Dzuba, V. V. Flambaum, and C. Harabati, *Phys. Rev. A* **84**, 052108 (2011).
- [17] H. J. Monkhorst, *Int. J. Quantum Chem.* **12**, 421 (1977).
- [18] N. C. Handy and H. F. Schaefer, *J. Chem. Phys.* **81**, 5031 (1984).
- [19] E. A. Salter, G. W. Trucks, and R. J. Bartlett, *J. Chem. Phys.* **90**, 1752 (1989).
- [20] H. Koch, J. Hans, J. Poul, T. Helgaker, G. E. Scuseria, and H. F. Schaefer III, *J. Chem. Phys.* **92**, 4924 (1990).
- [21] R. J. Bartlett and J. Noga, *Chem. Phys. Lett.* **150**, 29 (1988).
- [22] S. Pal, *Theor. Chim. Acta* **66**, 151 (1984).
- [23] R. J. Bartlett, S. A. Kucharski, and J. Noga, *Chem. Phys. Lett.* **155**, 133 (1989).
- [24] S. Pal, *Theor. Chim. Acta* **66**, 207 (1984).
- [25] J. Arponen, *Ann. Phys. (NY)* **151**, 311 (1983).
- [26] R. Bishop, J. Arponen, and P. Pajanne, *Aspects of Many-Body Effects in Molecules and Extended Systems* (Springer, Berlin, 1989).
- [27] S. Pal, *Phys. Rev. A* **34**, 2682 (1986).
- [28] P. G. Szalay, M. Nooijen, and R. J. Bartlett, *J. Chem. Phys.* **103**, 281 (1995).
- [29] C. Sur, R. K. Chaudhuri, B. K. Sahoo, B. P. Das, and D. Mukherjee, *J. Phys. B* **41**, 065001 (2008).
- [30] C. Sur and R. K. Chaudhuri, *Phys. Rev. A* **76**, 032503 (2007).
- [31] S. Sasmal, H. Pathak, M. K. Nayak, N. Vaval, and S. Pal, *Phys. Rev. A* **91**, 022512 (2015).
- [32] T. A. Isaev, S. Hoekstra, and R. Berger, *Phys. Rev. A* **82**, 052521 (2010).
- [33] T. Isaev and R. Berger, [arXiv:1302.5682](https://arxiv.org/abs/1302.5682).
- [34] A. D. Kudashov, A. N. Petrov, L. V. Skripnikov, N. S. Mosyagin, T. A. Isaev, R. Berger, and A. V. Titov, *Phys. Rev. A* **90**, 052513 (2014).
- [35] J. Cizek, *Correlation Effects in Atoms and Molecules*, Advances in Chemical Physics Vol. 14 (Wiley, New York, 1967).
- [36] S. Pal, M. D. Prasad, and D. Mukherjee, *Theor. Chim. Acta* **62**, 523 (1983).
- [37] S. Sasmal, H. Pathak, M. K. Nayak, N. Vaval, and S. Pal, *Phys. Rev. A* **91**, 030503 (2015).
- [38] M. G. Kozlov, V. Fomichev, Y. Y. Dmitriev, L. N. Labzovsky, and A. V. Titov, *J. Phys. B* **20**, 4939 (1987).
- [39] A. V. Titov, N. S. Mosyagin, A. N. Petrov, T. A. Isaev, and D. P. DeMille, *Progr. Theor. Chem. Phys.* **15**, 253 (2006).
- [40] L. R. Hunter, *Science* **252**, 73 (1991).
- [41] T. Saue *et al.*, DIRAC, a relativistic ab initio electronic structure program, release DIRAC10, 2010, <http://www.diracprogram.org>.
- [42] L. Visscher and K. Dyall, *At. Data Nucl. Data Tables* **67**, 207 (1997).
- [43] K. Faegri, Jr. and K. G. Dyall, *Introduction to Relativistic Quantum Chemistry* (Oxford University Press, New York, 2007).
- [44] K. G. Dyall, *J. Phys. Chem. A* **113**, 12638 (2009).
- [45] T. H. Dunning, *J. Chem. Phys.* **90**, 1007 (1989).
- [46] K. Wendt, S. A. Ahmad, W. Klempt, R. Neugart, E. W. Otten, and H. H. Stroke, *Z. Phys. D* **4**, 227 (1987).
- [47] W. Neu, R. Neugart, E. W. Otten, G. Passler, K. Wendt, B. Fricke, E. Arnold, H. J. Kluge, and G. Ulm, *Z. Phys. D* **11**, 105 (1988).
- [48] A. V. Titov, Y. V. Lomachuk, and L. V. Skripnikov, *Phys. Rev. A* **90**, 052522 (2014).
- [49] M. G. Kozlov and V. F. Ezhov, *Phys. Rev. A* **49**, 4502 (1994).
- [50] M. Kozlov, *J. Phys. B* **30**, L607 (1997).
- [51] A. V. Titov, N. S. Mosyagin, and V. F. Ezhov, *Phys. Rev. Lett.* **77**, 5346 (1996).
- [52] H. Quiney, H. Skaane, and I. Grant, *J. Phys. B* **31**, L85 (1998).
- [53] F. A. Parpia, *J. Phys. B* **31**, 1409 (1998).
- [54] N. Mosyagin, M. Kozlov, and A. Titov, *J. Phys. B* **31**, L763 (1998).
- [55] S. Sasmal, H. Pathak, M. K. Nayak, N. Vaval, and S. Pal, *J. Chem. Phys.* **144**, 124307 (2016).
- [56] H. M. Quiney, J. K. Laerdahl, K. Fægri, Jr., and T. Saue, *Phys. Rev. A* **57**, 920 (1998).
- [57] E. Lindroth, B. Lynn, and P. Sandars, *J. Phys. B* **22**, 559 (1989).